
Proceedings Paper:
Wareing, CJ, Falle, SAEG, Fairweather, M et al. (1 more author) (2014) RANS Modelling of Turbulent, Particle-Laden Sonic CO2 Jets. In: Proceedings of the 10th International ERCOFTAC Symposium on Engineering Turbulence Modelling and Measurements – ETMM10. 10th International ERCOFTAC Symposium on Engineering Turbulence Modelling and Measurements – ETMM10, 17-19 Sep 2014, Don Carlos Resort, Marbella, Spain. .

https://doi.org/10.1615/ichmt.2012.procsevintsympturbheattransfpal.350

RANS Modelling of Turbulent, Particle-Laden Sonic CO_2 Jets

C.J. Wareing[1, 2], S.A.E.G. Falle[1], M. Fairweather[2] and R.M. Woolley[2]

[1]School of Mathematics, University of Leeds, Leeds LS2 9JT, United Kingdom
[2]School of Process, Environmental and Materials Engineering, University of Leeds, Leeds LS2 9JT, United Kingdom

C.J.Wareing@leeds.ac.uk

1 Introduction

Carbon capture and storage (CCS) presents a short-term viable option for significantly reducing the amount of carbon dioxide (CO_2) released into the atmosphere from power generation and other large point sources, thereby mitigating the effects of climate change. Captured CO_2 will have to be transported between capture and storage locations, most likely along high pressure pipelines. Such pipelines require risk assessment considering the consequences of a pipeline puncture or rupture. Predicting the correct fluid phase and solid particle behaviour during such a discharge process in the near-field of sonic CO_2 jets is of particular importance in assessing this risk, given the very different hazard profiles of CO_2 in the gaseous and solid states. We have developed a fluid flow model for the near-field dispersion from high pressure liquid CO_2 pipelines (Wareing et al., 2013a), validating it against a range of experimental data at different scales from small punctures up to full-bore ruptures of 0.6 m pipelines (Woolley et al., 2013; Wareing et al., 2014).

Modifications to the model in order to predict solid particle behaviour have involved the incorporation of a Lagrangian particle tracker and particle distribution function (PDF). This has been applied to measurements of CO_2 jets (Wareing et al., 2013b), where particle sizes and velocities have been measured through Doppler techniques and agglomeration behaviour observed along the sonic jets. In that work, accompanying stand-alone numerical models successfully predicted the observed agglomeration behaviour. In the present work, we combine the different elements of the agglomeration model, particle tracker and PDF together and then further extend the numerical model with an improved turbulence model and an improved equation of state in order to more accurately model particle behaviour in sonic CO_2 jets, including non-equilibrium effects, viscous drag and particle evolution.

2 Previous work

Liu et al. (2012) examined the formation of solid CO_2 "dry ice" particles in a jet flow, with application to RESS cleaning processes. The particles were produced by the rapid expansion and cooling of supercritical CO_2 through a nozzle based on the Joule-Thomson effect. The experimental results showed that the primary dry ice particles ejected from the nozzle were about 1 micrometer in mass median diameter, measured through laser diffraction techniques. Agglomeration was observed initially along the sonic jet releases into a thermally insulated tube, followed by sublimation downstream. They considered the agglomeration process to be take place by the simultaneous processes of particle deposition and reentrainment; specifically agglomerated particles are reentrained from the layer of dry ice particles deposited on the tube walls. The agglomerate size was noted to decrease with increasing flow velocity, attributed to the greater detachment force applied to the deposition layer.

Recent similar experimental work by our group (Wareing et al., 2013b), applied to CCS scenarios rather than RESS cleaning, has shown that the initial liquid-breakup-formed particle distribution post Mach shock in a sonic liquid CO_2 release from high pressure into air is nozzle size independent and centred on a diameter of 1 to 2 micrometres, in agreement with Weber number predictions. Agglomeration has been detected in the free sonic CO_2 jet release with a 1.0 mm diameter nozzle, but not with a 0.5 mm diameter nozzle. One-dimensional numerical predictions were able to reproduce the observed agglomeration along the jet in the 1.0 mm case using a turbulent shear agglomeration approach.

To understand the lack of agglomeration in the 0.5 mm diameter case, our previous work considered the velocity measurements for each particle, recorded as part of the Doppler parti-

cle size measurements. In Figure 1, we reproduce the average magnitude of velocity for both the 0.5 mm diameter case (squares) and the 1.0 mm diameter case (circles). The centreline prediction of fluid mean velocity using our previous model (Wareing et al., 2013b) is also shown (line). The error bars indicate +/- 1σ of the distribution of particles at that location. The experimentally measured velocities are consistently similar at all distances, but not in agreement with the numerical prediction until 50 diameters (D) from the nozzle, indicating that the particles are out of equilibrium until 50D from the nozzle, at least on the centreline where the measurements were taken. Beyond 50D, the particle velocities track the fluid velocity, indicating particle-fluid equilibrium.

Theoretical calculations presented in Wareing et al. (2013b) indicated that for particles with a radius around 10^{-6} m (as observed), the dynamical relaxation time is 3×10^{-5} s at 200 K and 1.4×10^{-5} s at 280 K. At the nozzle exit, T~280 K and the velocity is approximately 100 m s^{-1}, so the stopping distance due to viscous drag is 1.4 mm. For the same particles, thermal relaxation times of 2.7×10^{-3} s at 200 K and 5.7×10^{-5} s at 280 K were calculated. At the nozzle exit with the same conditions, the relaxation distance to achieve thermal equilibrium was calculated to be 6.0 mm.

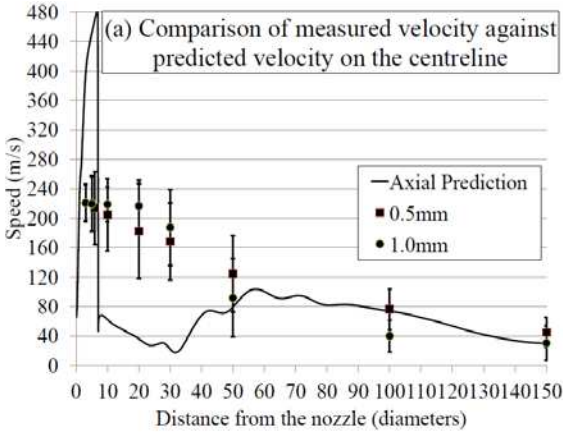

Figure 1. Experimental measurements of velocity (squares and circles) alongside numerical prediction of the centreline velocity in a sonic release.

The Mach shock in these sonic releases is at a distance of around 7 nozzle diameters along the centreline from the nozzle. In the case of a full scale CCS transport pipe (D~0.6 m), the Mach shock is approximately 4.2 m from the nozzle and as noted in our previous work, accounting for the viscous and thermal relaxation distances, the particles are likely to be reasonably close to equilibrium throughout the expansion and follow the flow. The flow accelerates from 100 m s^{-1} at the nozzle to around 450 m s^{-1} at the Mach shock over this 7D distance and it is likely that in full-scale releases, the particles will undergo this acceleration. However, for the small scale experimental releases considered here, the Mach shock is physically considerably close to the release point, 3.5 mm from the 0.5 mm diameter nozzle and 7 mm from the 1.0 mm diameter nozzle. The relaxation distances do not change and hence in these two cases particle inertia is not negligible and the particles are neither in dynamical nor thermal equilibrium throughout the initial part of the release. We note that the particles obtain their velocity through the explosive force of the release and by 50D, the experiments indicate they have approached equilibrium with the fluid and have a similar velocity.

In Figure 2, we reproduce the spread of the angle of the velocity vector away from the jet centreline from Wareing et al. (2013b). Again, the error bars indicate +/- 1σ of the distribution. The spread angle remains the same in the 0.5 mm diameter nozzle case, whilst increasing with distance along the jet in the 1.0 mm diameter nozzle case. This was taken in Wareing et al. (2013b) to indicate higher levels of turbulence in the 1.0 mm diameter nozzle jet. The particles are more likely to see turbulent structures and so the velocity variation reflects the increased level of turbulence in the 1.0mm diameter nozzle jet over the 0.5mm diameter nozzle. Inferring then from these results that the particles are seeing different levels of turbulence in the 1.0 mm nozzle case compared to the 0.5 mm nozzle case, we have set out to investigate whether turbulent shear agglomeration may be responsible for the agglomeration along the jet, which has required a complex numerical method, non-ideal thermodynamics and enhanced turbulence models.

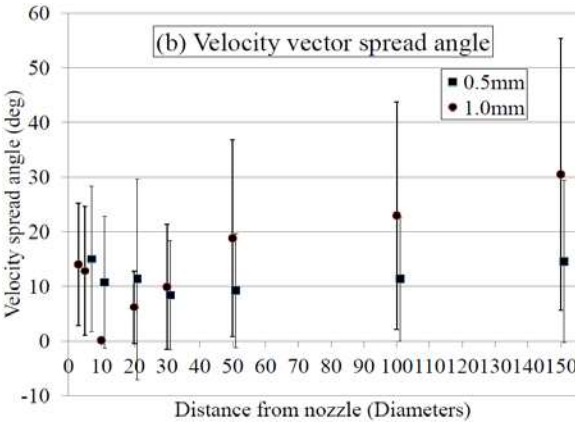

Figure 2. Experimental measurements of the velocity vector angle away from the jet centreline axis.

3 Numerical technique

We start from the numerical technique described in Wareing et al. (2013a) to predict the flow. In that technique, predictions are based on Reynolds-averaged Navier-Stokes (RANS) equation solutions of the density-weighted time-averaged (Favre) forms of the transport equations for mass, momentum and total energy, with closure of this equation set achieved using a suitable turbulence model. Solutions are obtained of the time-dependent, axisymmetric forms of the descriptive equations and the integration of the equations performed by a shock-capturing conservative, upwind second-order accurate Godunov numerical scheme (Falle, 1991). The fully-explicit, time-accurate, cell-centred finite-volume Godunov method is a predictor-corrector procedure, where the predictor stage is spatially first-order, and used to provide an intermediate solution at the half-timestep. This solution is then subsequently used at the corrector stage for the calculation of second-order accurate fluxes that lead to a second-order accurate cell-centred solution. A Harten, Lax, van Leer Riemann solver is employed to calculate fluxes at cell boundaries. The numerical scheme employs an unstructured adaptive mesh refinement (AMR) technique (Falle, 2005), requiring an order of magnitude less memory and giving an order of magnitude faster computation times than structured grid AMR. The two coarsest levels – 0 and 1 – cover the whole computational domain; finer grids need not do so. Refinement or derefinement depends on a given tolerance and automatically allows for finer resolution in the regions of strong gradients and lower resolutions elsewhere, as demonstrated in Figure 3. Defragmentation of the AMR grid in hardware memory is performed at every timestep, gaining further speed improvements for negligible cost through reallocation of cells into consecutive memory locations.

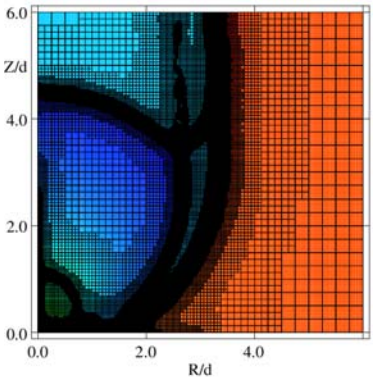

Figure 3. Automatic mesh refinement around gradients at a Mach shock in a high pressure release.

The numerical scheme employs a composite numerical equation of state method for CO_2. Previously our method employed the Peng-Robinson equation of state (Peng and Robinson, 1976) in the gas phase, look-up tables calculated from the Span and Wagner equation of state (Span and Wagner, 1996) in the liquid phase and for the saturation pressure, and data from the Design Institute for Physical Properties (DIPPR®) 801 database (www.aiche.org/ dippr/) for the latent heat of fusion and properties of the solid phase. For complete details please see Wareing et al. (2013a). An enhancement introduced here improves the treatment of the solid phase. Specifically, the Jager and Span equation of state (Jager and Span, 2012) is now used to more accurately model the solid phase, rather than DIPPR data as used previously. Our previous work (Wareing et al., 2013a) has shown that the low temperatures observed in these releases make it absolutely crucial to employ a three-phase equation of state to model near-field atmospheric dispersion of solid CO_2.

In Wareing et al. (2013b) we employed a compressibility corrected k-ε turbulence model. We have improved on this by the use of a more realistic Reynolds stress turbulence model (Jones and Musonge, 1988), modified in-line with recommendations made by Dianat et al. (1996) for round jets.

In Wareing et al. (2013b), we demonstrated that a turbulent shear agglomeration model dependent on the square root of ε (Saffman and Turner, 1956) can be used to evolve a particle distribution under the conditions found in such jets and is able to reproduce the observed agglomeration in the 1.0 mm diameter nozzle release. This result was obtained by calculating particle agglomeration alone under homogeneous turbulent conditions taken from such a jet release. We reproduce this result in Figure 4.

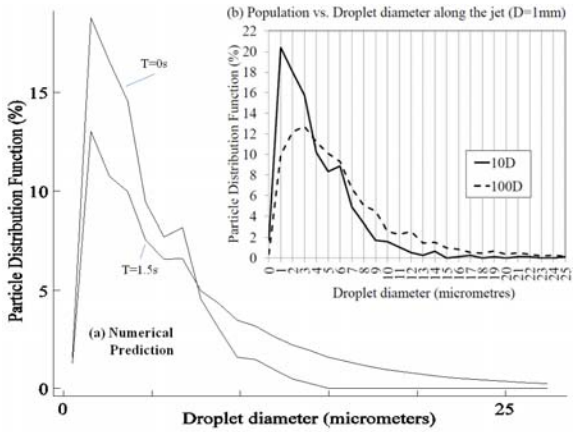

Figure 4. (a) Predicted turbulent shear agglomeration and (b) experimentally observed agglomeration with a 1.0 mm diameter nozzle.

We have now embedded this agglomeration model according to Saffman and Turner (1956):

$$\psi(r_1, r_2) = \eta_s \, \eta_e \, \chi_c^3 (r_1 + r_2)^3 \left(\frac{8 \rho_f \pi \varepsilon}{15 \mu} \right)^{1/2} \qquad (1)$$

into the particle evolution of the Lagrangian particle tracker in our numerical scheme, where η_s is the dimensionless particle to particle sticking efficiency, $\eta_e = \eta_e(r_1,r_2)$ is the dimensionless collision efficiency factor and χ_c is the dimensionless collisional shape factor. Hence we are now able to model agglomeration along the full jet and investigate whether turbulent shear can reproduce the agglomeration observed along the non-homogeneous sonic jet.

For more accurate representation of particle motion, accounting for equilibrium effects, we also include a viscous drag factor in the low Reynolds number limit calculation of particle velocity evolution in the Lagrangian particle tracker. The dynamic viscosity of CO_2 used is given by DIPPR as:

$$\mu = a_1 + a_2 T + a_3 T^2 \qquad (2)$$

where $a_1 = 1.12\times10^{-6}$, $a_2 = 4.98\times10^{-8}$ and $a_3 = -1.09\times10^{-11}$.

4 Results and discussion

In the numerical simulations presented below, homogeneous particles are injected at the nozzle (Z/d = 0, R/d <= 0.5) every 250 timesteps with the initial conditions presented in Wareing et al. (2013b). Specifically, they are given a velocity of 200 m s^{-1}, a radius of 1.5×10^{-6} m and a uniform density of 1500 kg m^{-3}. The Lagrangian particle tracker with evolution discussed in the previous section is then used to track the particles as they move through the fluid and monitor their evolution.

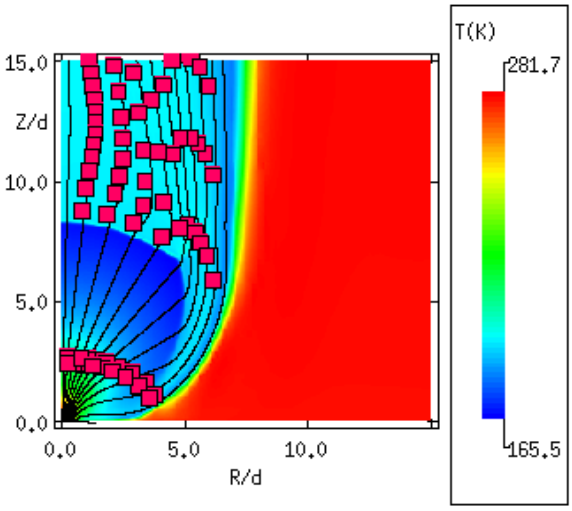

Figure 5. An axisymmetric temperature prediction of the near-field Mach shock structure with streamlines and red squares indicating particle locations.

In Figure 5 we show axisymmetric numerical predictions of the near-field particle behaviour in these small-scale jets obtained using a Reynolds stress second-moment closure turbulence model. The colour plot of temperature clearly shows the position of the Mach shock at 8D on the centreline. The temperature range in the expansion explicitly demonstrates the need for a three-phase accurate equation of state for CO_2, as the temperature goes far below 216.6K, the triple point temperature of CO_2. Streamlines are indicated through the flow by black lines. Particles, introduced at an earlier time at regular intervals at the origin are now moving through the flow, their location indicated by solid red squares in this plot. It should be noted that they are not explicitly following the streamlines as the viscous drag is having an effect on their motion.

In Figure 6 we show the larger domain from the release point up to 70D from the nozzle along the centreline. The solid particles keep the jet cold along the length presented here. Again, black lines indicate stream lines and particle locations are indicated by red squares. By 50D, the particles are now moving along the streamlines, which would agree with the observations in Figure 1, where particles reach (velocity) equilibrium with the fluid after ~50D.

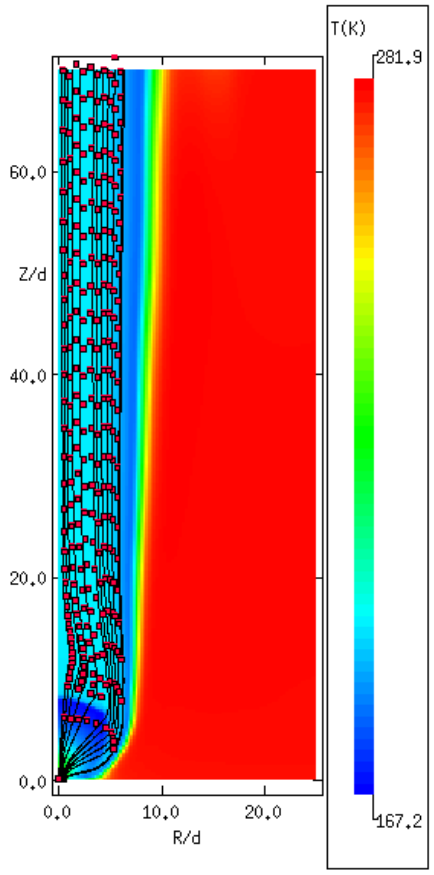

Figure 6. An axisymmetric temperature prediction of the jet structure with streamlines and red squares indicating particle locations.

To further confirm velocity equilibrium, we show the fluid velocity and the particle velocities in Figure 7. The predicted centreline velocity of the fluid decreases from 120 m s^{-1} at 40D to under 100 m s^{-1} at 120D. It should be noted that the particle velocities, as indicated by the colour of the squares, appear to show exactly the same behaviour and there is good agreement with fluid flow velocity throughout this region, as observed in the experiments (see Figure 1).

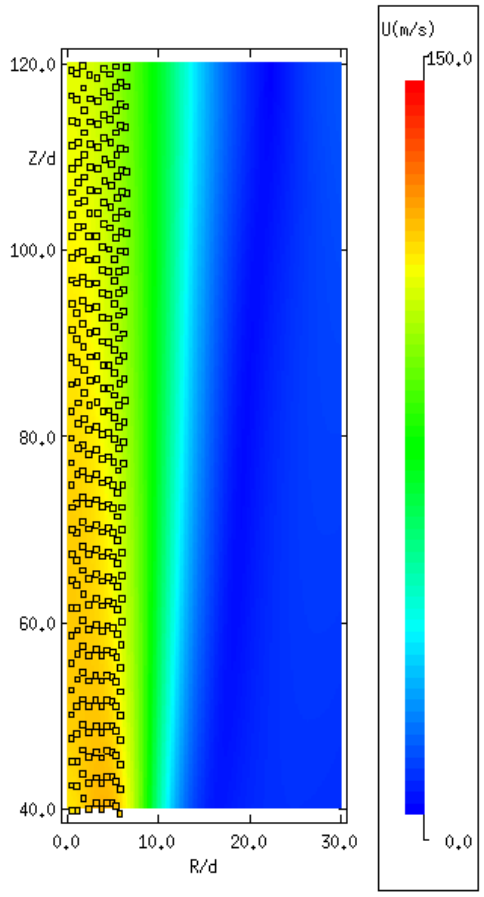

Figure 7. An axisymmetric velocity prediction of the far-field jet structure with squares indicating particle locations and the colour of the squares indicating the particle velocity on the scale presented.

Finally, in Figure 8, we show the variation of particle mass along the jet. Given that the particles are all injected at the nozzle at regular intervals with the same radius and density and hence the same mass, there is mass change predicted along the jet. In the current numerical scheme, the only mechanism for mass change is agglomeration driven by turbulent shear (Saffman and Turner, 1956). The particle masses beyond 100D on the centreline indicate radii around 3-4 micrometers, which is in good agreement with the shift of the peak of the distribution in Panel (b) of Figure (4). Hence, turbulent shear agglomeration predicted in a sonic CO_2 jet is able to reproduce experimentally observed agglomeration. It should also be noted that much larger particles are generated at the edges of the jet. In these regions the levels of turbulence are greater and hence drive greater rates of agglomeration. The experiments are unable to confirm this prediction, as particle sizes and velocities were only measured on the centreline of the sonic jet. Future experiments hope to make observations at radial cuts across the jet and test this prediction.

5 Concluding remarks

Particles of solid CO_2 are generated through the rapid expansion and cooling in a sonic jet formed from a release from a high pressure liquid reservoir through a small diameter nozzle. Such particles have previously been found (Wareing et al., 2013b) to initially be in neither dynamical equilibrium nor thermal equilibrium with the sonic flow. By 50 nozzle diameters or so along the jet, previous experiments have indicated they are in equilibrium with the fluid. Particle agglomeration along such jets has also been noted (Liu et al., 2012; Wareing et al. 2013b).

Numerical studies of fluid flow in axisymmetric jets with Lagrangian particle tracking techniques presented herein have demonstrated that by using an appropriate turbulent shear agglomeration model and accounting for equilibrium effects through CO_2 temperature dependent viscous drag in the calculation of particle motion, it is possible to model particle movement and evolution in such sonic CO_2 jets and reproduce the experimental observations referred to above. This numerical modelling requires a complete three-phase accurate equation of state and a high fidelity turbulence model with refinements for sonic jets.

These issues are highly important for high pressure releases of CO_2 through small nozzles, such as RESS cleaning processes and fracking processes. They are also important for CO_2 transport in CCS scenarios, in particular for small pipeline puncture but have less of a bearing for larger-scale punctures and ruptures where the release diameter could be up to the pipeline diameter (~1m) in the case of a full bore rupture. Nevertheless, particle behaviour in such releases should be accounted for in order to estimate how much CO_2 remains in and around the puncture or rupture site.

We plan to extend the model to supercritical releases, modelling available experimental data (Liu et al., 2012) and further apply the model to cleaning processes involving the rapid expansion of supercritical solutions. Further, the effects of impurities will be examined.

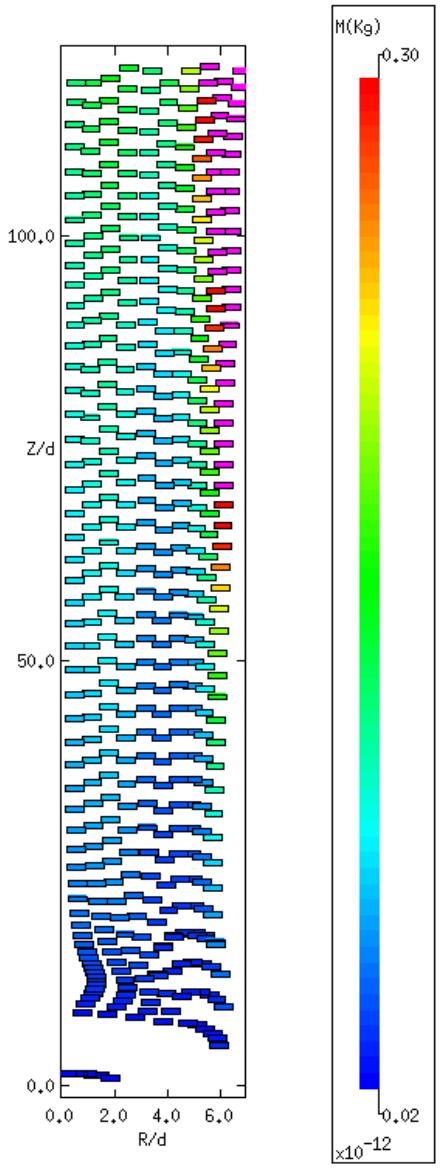

Figure 8. Particle masses along the sonic CO_2 jet. Agglomeration, due to turbulent shear, is indicated by the colour change of the squares.

References

Dianat, M., Fairweather, M. and Jones, W.P. (1996), Reynolds stress closure applied to axisymmetric impinging turbulent jets, *Theor. Comp. Fluid Dynamics*, Vol. 8, pp. 435-447.

Falle, S.A.E.G. (1991), Self-similar jets, *Mon. Not. R. Astron. Soc.*, Vol. 250, pp. 581-596.

Falle, S.A.E.G. (2005), AMR applied to non-linear elastodynamics, *Adaptive Mesh Refinement – Theory and Applications; Lecture Notes in Computational Science and Engineering*, Vol. 41, pp. 235-253.

Jager, A. and Span, W. (2012), Equation of state for solid carbon dioxide based on the Gibbs free energy, *J. Chem. Eng. Data*, Vol. 57, pp. 590-597.

Jones, W.P. and Musonge, P. (1988), Closure of the Reynolds stress and scalar flux equations. *Phys. Fluids*, Vol. 31, pp. 3589-3604.

Liu, Y., Calvert, G., Hare, C., Ghadiri, M. and Matsusaka, S. (2012), Size measurement of dry ice particles produced from liquid carbon dioxide, *J. Aerosol Sci.*, Vol. 48, pp. 1-9.

Peng, D.-Y. and Robinson, D.B. (1976), A new two-constant equation of state, *Ind. Eng. Chem. Fundam.*, Vol. 15, pp. 59-64.

Saffman, P.G. and Turner, J.S. (1956), On the collision of drops in turbulent clouds, *J. Fluid Mech.*, Vol. 1, pp. 16-30.

Span, R. and Wagner, W. (1996), A new equation of state for CO_2 covering the fluid region from the triple-point temperature to 1100K and pressures up to 800 MPa, *J. Phys. Chem. Ref. Data.*, Vol. 25, pp. 1509-1596.

Wareing, C.J., Woolley, R.M., Fairweather, M. and Falle, S.A.E.G. (2013a), A composite equation of state for the modelling of sonic carbon dioxide jets in carbon capture and storage scenarios, *AIChE J.*, Vol. 59, pp. 3928-3942.

Wareing, C.J., Fairweather, M., Peakall, J., Keevil, G., Falle, S.A.E.G. and Woolley, R.M. (2013b), Numerical modelling of particle-laden sonic CO_2 jets with experimental validation, *AIP Conference Proceedings*, Vol. 1558, pp. 98-102.

Wareing, C.J., Woolley, R.M., Fairweather, M. and Falle, S.A.E.G. (2014), Validation of a model of gas and dense phase CO_2 jet releases for carbon capture and storage application, *Int. J. Greenh. Gas Con.*, Vol. 20, pp. 254-271.

Woolley, R.M., Fairweather, M., Wareing, C.J., Falle, S.A.E.G., Proust, C., Hebrard, J. and Jamois, D. (2013), Experimental measurement and Reynolds-averaged Navier-Stokes modelling of the near-field structure of multi-phase CO_2 jet releases, *Int. J. Greenh. Gas Con.*, Vol. 18, pp. 139-149.